GDCh
Communication
Angewandte Chemie International Edition
www.angewandte.org

How to cite: *Angew. Chem. Int. Ed.* **2024**, *63*, e202404539
doi.org/10.1002/anie.202404539

Covalent Organic Frameworks | Hot Paper

Mechanochemical Synthesis of Boroxine-linked Covalent Organic Frameworks

Ehsan Hamzehpoor⁺, Farshid Effaty⁺, Tristan H. Borchers, Robin S. Stein, Alexander Wahrhaftig-Lewis, Xavier Ottenwaelder, Tomislav Friščić,* and Dmytro F. Perepichka**

Abstract: We report a rapid, room-temperature mechanochemical synthesis of 2- and 3-dimensional boroxine covalent organic frameworks (COFs), enabled by using trimethylboroxine as a dehydrating additive to overcome the hydrolytic sensitivity of boroxine-based COFs. The resulting COFs display high porosity and crystallinity, with COF-102 being the first example of a mechanochemically prepared 3D COF, exhibiting a surface area of *ca.* 2,500 $m^2 g^{-1}$. Mechanochemistry enabled a >20-fold reduction in solvent use and ~100-fold reduction in reaction time compared with solvothermal methods, providing target COFs quantitatively with no additional work-up besides vacuum drying. Real-time Raman spectroscopy permitted the first quantitative kinetic analysis of COF mechanosynthesis, while transferring the reaction design to Resonant Acoustic Mixing (RAM) enabled synthesis of multi-gram amounts of the target COFs (tested up to 10 g).

Since the pioneering report in 2005,[1] crystalline two- and three-dimensional[2] (2D and 3D, respectively) porous covalent organic frameworks (COFs) have emerged as a distinct class of organic materials with enticing properties and applications.[3] Boroxine is the first and among the simplest synthons used in COF design, providing materials widely studied for applications in gas sorption, hydrogen isotope separation, semiconductors, and, recently, room-temperature phosphorescent sensors.[4] Boroxine linkers are formed by condensation of three boronic acid groups (one per monomer) in a highly dynamic process that enables error correction during polymerization. This reversible condensation thus promotes the formation of highly ordered materials,[4d] but is also the cause of their poor hydrolytic stability.[5,6]

Boroxine-linked COFs are typically obtained by solvothermal synthesis, which involves heating pressurized solutions of multifunctional boronic acids at temperatures $>100\,°C$ for extended periods of time.[2,4d,7] To date, only a few modifications to the original solvothermal synthetic approach have been reported: sonochemical synthesis,[8] Lewis-base-catalyzed room-temperature synthesis,[9] and, recently, transesterification-condensation of arylboronic esters using methylboronic acid (MBA) auxiliary under solvothermal conditions.[10]

Mechanochemistry,[11] which employs mechanical force such as grinding, milling and extrusion[12] for chemical transformations, has emerged as a versatile, "green" method for the synthesis of organic,[13,14] biomolecular,[15] and inorganic materials.[16] It can dramatically reduce the amount of chemical waste generated during the industrial production of chemicals and materials,[13] 90 % of which is from using solvents.[17] Mechanochemistry can also achieve higher yields, reaction rates, and different reactivity patterns than those seen in solution.[18] In particular, Resonant Acoustic Mixing (RAM) has recently emerged as a particularly attractive method for mechanochemical synthesis due to its high potential for scalability. RAM enables a direct input of mechanical energy to the sample, which eliminates the need for milling media, such as balls or screws, that are otherwise ubiquitous in conventional mechanochemical methods. This allows scalable mechanochemical transformations and minimizes the risk of sample contamination due to leaching or abrasion of milling media.[18]

---

[*] Dr. E. Hamzehpoor,⁺ F. Effaty,⁺ Dr. R. S. Stein, Prof. T. Friščić, Prof. D. F. Perepichka
Department of Chemistry
McGill University
801 Sherbrooke St. W., Montreal, H3A 0B8 (Canada)
E-mail: t.friscic@bham.ac.uk
dmytro.perepichka@mcgill.ca

F. Effaty,⁺ Prof. X. Ottenwaelder
Department of Chemistry and Biochemistry
Concordia University
7141 Sherbrooke St. W., Montreal, H4B 1R6 (Canada)
E-mail: Dr.X@concordia.ca

F. Effaty,⁺ Dr. T. H. Borchers, Dr. A. Wahrhaftig-Lewis, Prof. T. Friščić
School of Chemistry
University of Birmingham
Edgbaston, Birmingham, B15 2TT (United Kingdom)

Dr. R. S. Stein
Bruker UK Ltd
Longwood Close, Westwood Business Park, Coventry, CV4 8HZ (United Kingdom)

[⁺] Equal contribution.

While mechanosynthesis of metal–organic frameworks (MOFs) has been extensively studied for almost two decades,[16a,b,18d,19] applications of mechanochemistry to COFs have remained much less developed. In 2013, Banerjee group pioneered the mechanosynthesis of imine/ketoenamine-linked COFs by grinding the corresponding monomers in a mortar. The crystallinity and porosity of mechanochemically synthesized COFs are, however, generally lower than for solvothermally synthesized analogues.[20] While the use of liquid additives (liquid-assisted grinding, LAG) can improve the crystallinity of mechanochemically synthesized COFs, the accessible porosity is, in most cases, lower than in solvothermally synthesized COFs.[21] Recently, Borchardt and co-workers reported the first mechanosynthesis of triazine-linked COFs using triflic acid-catalyzed cyclotrimerization of nitriles.[22a] All other mechanochemical syntheses of COFs involve imine/keto-enamine condensations,[20–22] wherein the high hydrolytic stability of imine bonds allows the framework assembly in the presence of water, the reaction by-product. In contrast, the low hydrolytic stability of boroxine links and a near-unity equilibrium constant[23] make the mechanochemical synthesis of boroxine COFs challenging.

Here, we show how this challenge can be overcome by using trimethylboroxine (TMB) as both a water-scavenging agent and a modulator, enabling the first mechanochemical synthesis of boroxine-linked COFs (Scheme 1). We first used COF-1 as a model for the in-depth study of this polymerization reaction by ball-milling or RAM. In each case, a series of experiments was performed to find the best ratio of reactants and liquid additives to optimize reaction time and COF crystallinity. In the ball-milling method under herein optimized conditions (Entry S1, Table S2), a 10 mL zirconia milling jar was equipped with a zirconia ball (10 mm diameter, 3.7 g), loaded with 50 mg of 1,4-phenylenediboronic acid (PBA), TMB (2.0 equiv.) and a small amount of a 1:1 (v/v) mixture of mesitylene (Mes) and dioxane (or Mes and THF) (expressed by the ratio of liquid additive to reaction mixture weight,[24] $\eta = 0.8\ \mu L\,mg^{-1}$), and milled at 25 Hz for 30 minutes. Under optimized RAM conditions (Entries S50–S62, Table S5–6), commercial glass vials (volume of 4 mL, 20 mL, or 100 mL, depending on the reaction scale) were charged with the same reagents and liquid additives, and reactions performed for 3 h at an acceleration of 90 g (where $g = 9.81\ m\,s^{-2}$), yielding from 50 mg up to 10 g of crystalline COF-1 (Figure S23). The obtained COF powder from each method was then dried under reduced pressure (1 h, 50 °C, ~50 Torr) to afford samples designated as COF-1_{BM} and COF-1_{RAM} without any further purification.[25]

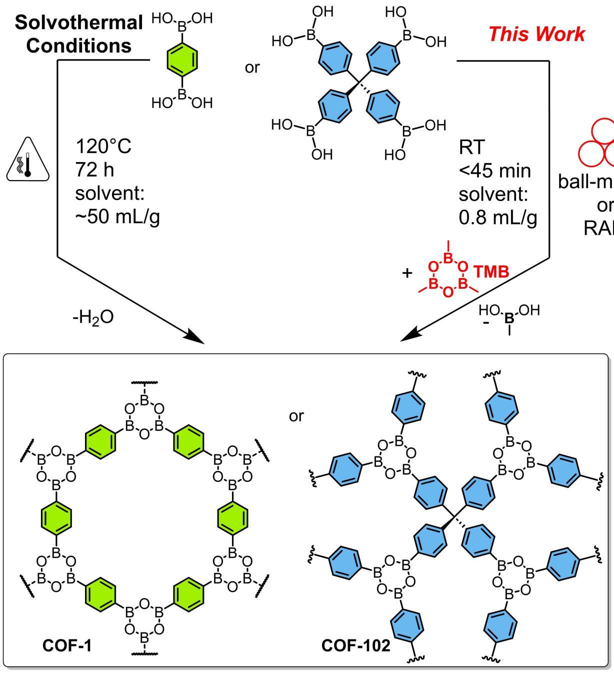

Scheme 1. Conventional solvothermal vs herein reported TMB-mediated mechanochemical synthesis of boroxine COFs. Symbol for mechanochemical reaction adopted from Rightmire & Hanusa.[27]

The role of each component in the COF-1_{BM} synthesis was studied in a series of control experiments (Tables S2–4) wherein the degree of polymerization and COF crystallinity were assessed by infrared (IR) spectroscopy (following the characteristic boroxine band) and powder X-ray diffraction (PXRD), respectively. Neat grinding (Entry S2) or LAG (Mes/THF mixture as a liquid additive, Entry S3) of PBA in the absence of TMB did not lead to any boroxine formation, likely due to the reversibility of boroxine linkage formation in the presence of water.[5] Using other dehydrating agents, such as $MgSO_4$ (Entry S5) or triphenylboroxine (TPB, Entry S6), led to boroxine formation, but no PXRD signals from COF-1 were observed (Figure S7). No condensation occurred when MBA was used instead of TMB (Entry S4). These results suggest that TMB not only shifts the equilibrium as a dehydrating agent but also facilitates the growth of a crystalline COF material. We speculate that TMB regulates the formation of an ordered polymer through the controlled release of intermediates (mixed aryl/methyl boroxines), akin to a similar modulating effect of aniline on the growth of imine COFs from diaminoarene monomers.[26] Varying the stoichiometry of TMB from 0.5-3.0 equivalents (Entry S7–S10) shows that two equivalents (1 molecule of TMB per boronic acid unit) is required for the complete conversion of the PBA monomer to the COF.

In the absence of liquid additives (Entry S11), only a partial conversion of boronic acid to COF-1 was achieved, even with three equivalents of TMB and longer milling times (Entry S12). The presence of *both* polar (THF or dioxane) and aromatic (Mes) liquid additives seems essential. When only one of these is used, the reaction is either too slow (Mes as a LAG additive, Entry S13) or yields a COF with poor crystallinity (THF as a LAG additive, Entry S14). These observations suggest that the polar liquid likely promotes the mobility of the PBA monomer, while mesitylene might exhibit a framework-templating effect as proposed earlier.[1,22b]

The IR and PXRD data for COF-1_{BM} and COF-1_{RAM} are very similar to those of the solvothermally synthesized COF-1_{Solv} (Figure 1a–b).[1] The disappearance of the OH-stretch

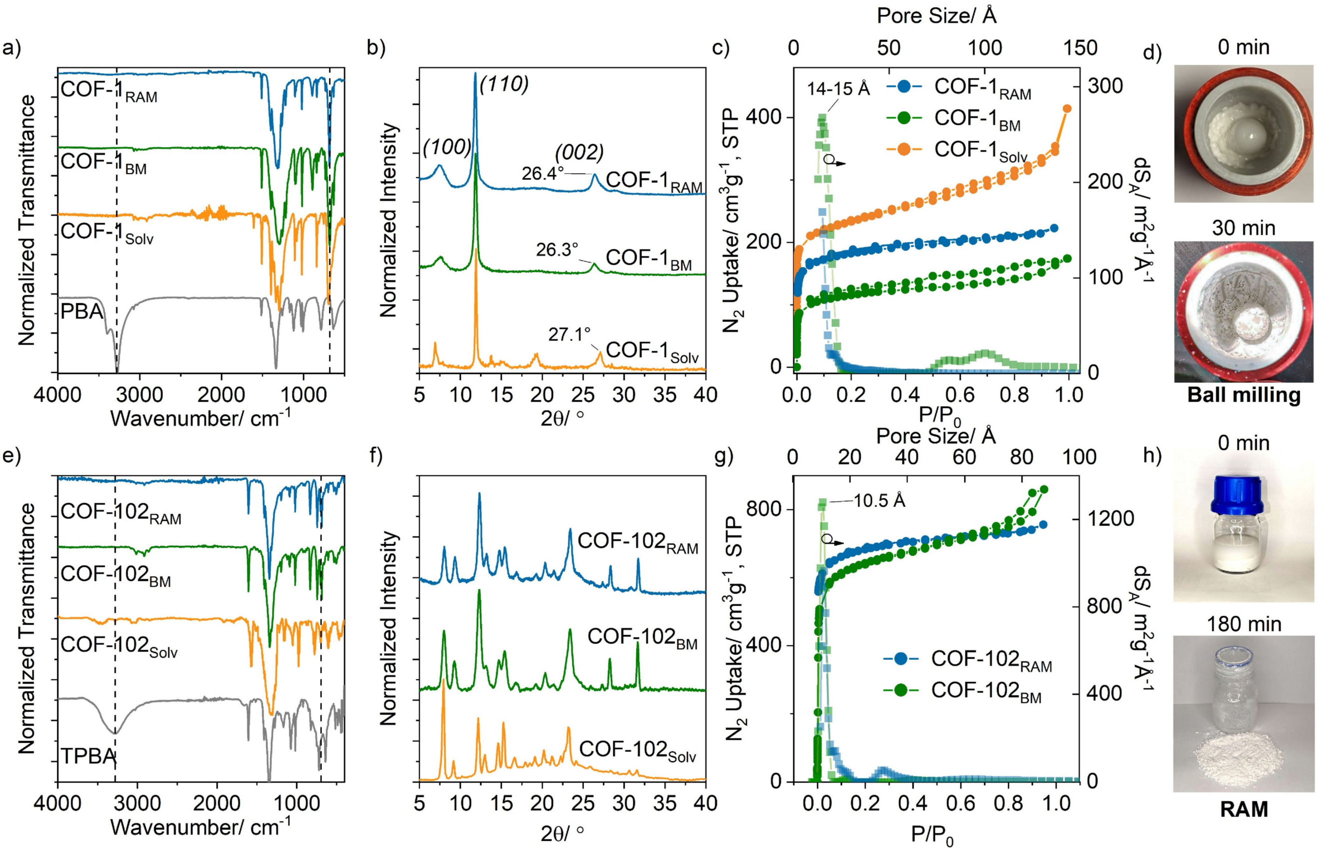

Figure 1. (**a**) IR spectra for COF-1_{BM}, COF-1_{RAM}, COF-1_{Solv} and PBA (precursor). (**b**) PXRD patterns of COF-1_{BM}, COF-1_{RAM}, and COF-1_{Solv}. (**c**) N_2 adsorption isotherms (left axis) for COF-1_{BM}, COF-1_{RAM}, and COF-1_{Solv} and pore size distribution (right axis) for COF-1_{BM} and COF-1_{RAM}. (**d**) Photographs of the COF-1_{BM} reaction mixture before and after ball-milling. (**e**) IR spectra for COF-102_{BM}, COF-102_{RAM}, COF-102_{solv} and TPBA (precursor). (**f**) PXRD patterns for COF-102_{BM}, COF-102_{RAM}, COF-102_{Solv}. (**g**) N_2 adsorption isotherm (left axis) and pore size distribution (right axis) analysis of COF-102_{BM} and COF-102_{RAM}. (**h**) Photographs of the large scale (10 g) reaction mixture of COF-1_{RAM} before and after RAM. IR and PXRD data for the solvothermally-synthesized COF-102_{Solv} in (e and f) are re-plotted from ref [2a]. The dashed lines in (a) and (e) show the position of the OH stretch of the -B(OH)$_2$ group and the out-of-plane bending of the B_3O_3 ring.

(3200-3400 cm^{-1}) and the emergence of a B_3O_3 out-of-plane ring bending (680 cm^{-1}) indicate the transformation of the boronic acid into boroxine links. Analysis of COF-1_{BM} and COF-1_{RAM} by PXRD shows the same Bragg reflections at $2\theta = 6.8°$ (100), 11.7° (110), and 27.1° (002) as COF-1_{Solv} (Figure 1b). The larger full width at half maximum (FWHM) value for the (110) reflection and the fewer diffraction signals in COF-1_{BM} and COF-1_{RAM} suggest smaller crystalline domains as compared to COF-1_{Solv}. Upon longer milling the ratio of intensities of (100) and (110) reflections increases, which can be ascribed to a previously studied phase transition in COF-1 (Figure S9).[1,29]

The Brunauer–Emmett–Teller (BET) analysis of the nitrogen sorption isotherm at 77 K (Figure 1c) of activated COFs obtained by vacuum drying (10^{-3} Torr, 160 °C, 12 h), reveals that COF-1_{RAM} and COF-1_{BM} exhibit SA_{BET} of 680 m^{2}g^{-1} and 445 m^{2}g^{-1}, respectively. Although these values are 8 % and 40 % lower than the 740 m^{2}g^{-1} for COF-1_{Solv} (Figure S2, Table S1), they still compare favorably to the reported surface areas of most mechanochemically-synthesized COFs.[22] The reduction in surface area may be caused by entrapment of TMB and/or random slippage of the layers in COF-1_{BM} and COF-1_{RAM}, consistent with the increase of the interlayer distance based on the position of the (002) reflection in the PXRD pattern (d-spacing 3.38 Å in COF-1_{BM} and 3.37 Å in COF-1_{RAM} vs. 3.29 Å in COF-1_{Solv}). Nevertheless, the pore size distribution obtained from the quenched-solid density functional theory (QS-DFT) of the N_2 isotherm data for both COF-1_{BM} and COF-1_{RAM} correspond closely to the micropore dimensions expected for COF-1[1] with minor contributions of mesopores at ~30–60 Å in the COF-1_{BM}.

Scanning electron microscopy (SEM, Figures 2a, S3) images reveal large (tens of microns), sponge-like particles of COF-1_{BM}, as opposed to the sub-micron particles of COF-1_{Solv} (Figure 2b). This unusual morphology is likely the result of a combination of particle aggregation due to mechanical impact during ball milling and the evaporation of liquid additives and MBA from the compacted particles. In contrast, COF-1_{RAM} particles show a nanopowder morphology similar to the COF-1_{Solv} (Figure 2c).

Solid-state Cross-Polarization Magic Angle Spinning (CP-MAS) ^{13}C NMR spectra of COF-1_{RAM} and COF-1_{BM} are very similar to that of COF-1_{Solv} (Figure S4) and are

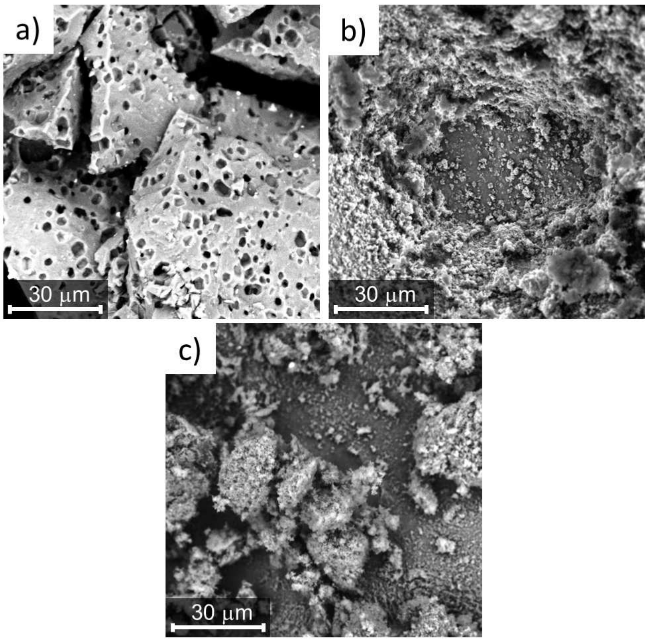

Figure 2. SEM images of the (a) COF-1_{BM} obtained via ball-milling (Entry S1, Table S2), (b) COF-$1_{Solv,}$ and (c) COF-1_{RAM} obtained via RAM (Entry 15, Table S2).

dominated by the aromatic C(H) carbon at 134 ppm. Different from COF-1_{Solv}, they also show a minor additional signal at -1 ppm attributed to a methyl group of methylboroxine. FSLG-HETCOR experiment (Figure S5) shows that this group is in close contact with the benzene ring carbons and we assign it to the -CH_3 end-groups at the edges of the polymer sheets of the COF.

We then applied mechanochemical ball-milling and RAM methods to the condensation of methanetetrayltetrakis(benzeneboronic acid) (Entry S63–65, Table S7), resulting in the formation of products designated as COF-102_{BM} and COF-102_{RAM}, respectively. While mechanosynthesis of 3D-MOFs is well-established,[16a,b,18d,19] this represents, to the best of our knowledge, the first mechanosynthesis of a 3D-COF. The COF-102_{BM} and COF-102_{RAM} products show consistent and similar IR signals, PXRD data (Figures 1e–f) and surface area (Figure 1g; SA_{BET} 2475 $m^2 \cdot g^{-1}$ and 2640 $m^2 \cdot g^{-1}$ for COF-102_{BM} and COF-102_{RAM}, respectively) as for the reported COF-102_{Solv} (~2600–3470 $m^2 \cdot g^{-1}$).[2a,30] It suggests that, unlike the 2D-COFs in which mechanical impact can block the pores via slippage of 2D sheets, the rigid 3D-COF scaffold is less disrupted during mechanosynthesis.

Kinetic analysis of COF formation is important to understand the growth mechanism and optimize reaction parameters.[10,22b,31] The kinetics of COF-1_{BM} formation by ball milling was studied by ex situ IR spectroscopy (Figures 3a, S9–10 and S19, Table S3), revealing that the reaction reaches completion within ~45 min at a milling frequency of 25 Hz, with an initial reaction rate R_0 ~6.7×10^{-3} s^{-1} (i.e., 0.67 % conversion per second, Figure 3a). PXRD analysis of the COF product at different time intervals also shows a decrease in the intensity of reflections corresponding to PBA during milling (Table S3, Entries S23–32). The crystallinity of COF-1_{BM} remains largely constant ($FWHM_{(100)}$ 0.2–0.3°) for up to 45 min milling time but starts to decrease upon longer milling ($FWHM_{(100)}$ 0.61° at 90 min), which suggests mechanical damage to the COF by the milling process and highlights the importance of optimizing reaction conditions and time.

We also examined the influence of ball milling frequency (5–30 Hz) on the formation of COF-1 after 10 and 45 min of milling (Table S4). Increasing the milling frequency accelerates the reaction (Figure 3b), consistent with higher energy input and more rapid mixing, but does not significantly affect COF crystallinity (Figures S11–12, Table S4).

Raman spectroscopy was used for in situ monitoring of the RAM synthesis of COF-1 (Figure S19–21).[32] The resulting data provided the first real-time spectroscopic insight into mechanochemical COF formation, revealing the formation of the boroxine ring (evidenced by a band at 673 cm^{-1}) and depletion of the boronic acid (evidenced by a band at 1100 cm^{-1}) over the course of 3 h (Figures 3c,d). Both the formation of COF-1_{RAM} and consumption of PBA were found to follow first-order kinetics with a rate constant of ca. $(3.4 \pm 0.2) \times 10^{-4}$ s^{-1} under the optimized RAM reaction (Figures 3d, S22). The initial rate for COF-1_{RAM} formation under these conditions is 3.1×10^{-4} s^{-1}, illustrating the ~20 times slower initial reaction kinetics under the softer RAM conditions compared with ball-milling. Under softer RAM conditions, the crystallinity remained almost unchanged with only 0.06° increase in $FWHM_{(100)}$ after 2 h of agitation.

In summary, this study introduces the first mechanochemistry-based, scalable synthetic method for boroxine-linked 2D and 3D COFs. Mechanosynthesis in the presence of TMB as a dehydrating agent provided model frameworks COF-1 and COF-102 as materials with similar spectroscopic characteristics and comparable surface areas to their solvothermally synthesized counterparts. Isolation of the materials by our method requires no work-up besides vacuum-evaporating the volatiles (liquid additives and TMB). The herein-reported optimized synthesis of COF-102 represents the first example of a mechanochemically obtained 3D COF featuring a remarkably high surface area of >2600 $m^2 g^{-1}$. By using RAM, the solvent-free synthesis of COF-1 was readily scaled from hundreds of milligrams up to 10 grams.[18c] The real-time Raman spectroscopy monitoring permitted in situ study of the reaction kinetics, and showed ca. 20-fold difference in reaction rates between the RAM and the ball-milling processes. The bespoken traits of mechanosynthesis and the observed properties of the produced COFs from this method, present potential solutions to the current challenges in making COFs, such as synthetic inefficiency (large solvent and energy waste) or the reliance on the solubility of precursors.[33,10]

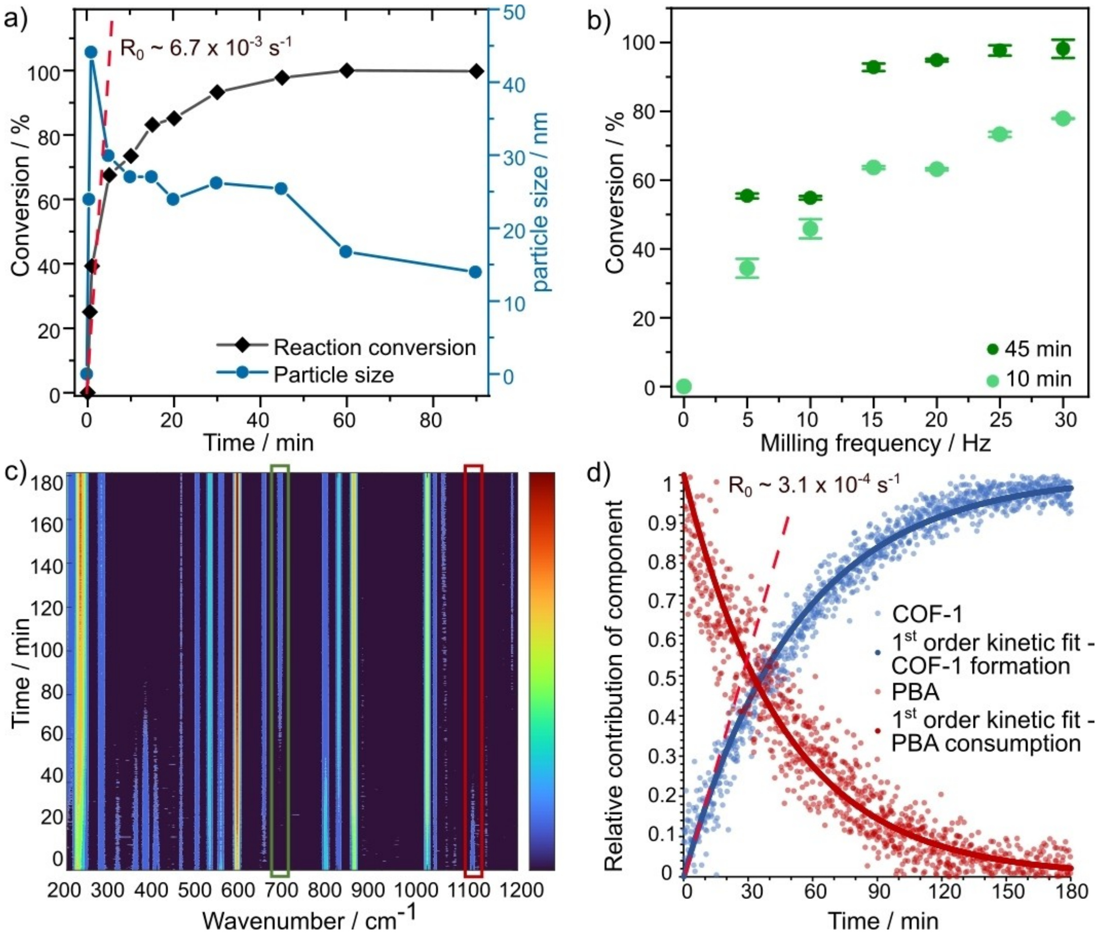

Figure 3. (**a**) The kinetic plot of COF-1_{BM} formation at 25 Hz and correlated particle size, obtained from the Scherrer analysis for the (110) Bragg reflection of COF-1 at $2\theta = 11.9°$, indicating a decrease of particle size upon ball-milling and reaction progress. (**b**) Reaction progress vs. milling frequency after 10 and 45 min. The conversion percentages are calculated using quantitative IR analysis, with the error bars obtained from different calibration curves for the same sample. For reaction conditions, see Entries S15–36 in the SI. (**c**) In-situ Raman spectroscopy monitoring of the synthesis of COF-1_{RAM} (see Figure S20 for Raman spectra of individual components). Selected bands for the formation of COF-1_{RAM} and consumption of PBA are highlighted in the green and red boxes respectively. (**d**) Changes in the intensity of Raman bands corresponding to a decrease of PBA (red plot, monitored at 1100 cm^{-1}) and formation of COF-1 (blue plot, monitored at 673 cm^{-1}). The scattered data in (d) results from changes in the intensity of Raman scattering during RAM agitation of the vial. For the corresponding first-order kinetics fit, see Figure S21.

Acknowledgements

This work was supported by NSERC Discovery Grants (to X.O., T.F. and D.F.P.). E.H. and F.E. acknowledge FRQNT doctoral scholarships. We are grateful to the McGill Chemical Characterization Facility (MC2), the McGill Institute for Advanced Materials (MIAM), Concordia's Centre for Nanoscience Research, the Leverhulme International Professorship (T.F.), University of Birmingham School of Chemistry, and facilities accessible at the Birmingham Centre for Mechanochemistry. We thank C. B. Lennox and J. Vainauskas for valuable discussions.

Conflict of Interest

The authors declare no conflict of interest.

Data Availability Statement

The data that support the findings of this study are available in the supplementary material of this article.

Keywords: Mechanochemistry · Covalent Organic Frameworks · Porous Material · Resonant Acoustic Mixing · Boroxines

---

[1] A. P. Côté, A. I. Benin, N. W. Ockwig, M. O'Keeffe, A. J. Matzger, O. M. Yaghi, *Science* **2005**, *310*, 1166–1170.

[2] a) H. M. El-Kaderi, J. R. Hunt, J. L. Mendoza-Cortés, A. P. Côté, R. E. Taylor, M. O'Keeffe, O. M. Yaghi, *Science* **2007**, *316*, 268–272; b) D. Beaudoin, T. Maris, J. D. Wuest, *Nat. Chem.* **2013**, *5*, 830–834.

[3] a) K. Geng, T. He, R. Liu, S. Dalapati, K. T. Tan, Z. Li, S. Tao, Y. Gong, Q. Jiang, D. Jiang, *Chem. Rev.* **2020**, *120*, 8814–8933; b) N. Huang, P. Wang, D. Jiang, *Nat. Rev. Mater.* **2016**, *1*, 16068; c) S. Kandambeth, K. Dey, R. Banerjee, *J. Am. Chem.

Soc. **2019**, *141*, 1807–1822; d) X. Liu, D. Huang, C. Lai, G. Zeng, L. Qin, H. Wang, H. Yi, B. Li, S. Liu, M. Zhang, R. Deng, Y. Fu, L. Li, W. Xue, S. Chen, *Chem. Soc. Rev.* **2019**, *48*, 5266–5302.

[4] a) H. Furukawa, O. M. Yaghi, *J. Am. Chem. Soc.* **2009**, *131*, 8875–8883; b) H. Oh, S. B. Kalidindi, Y. Um, S. Bureekaew, R. Schmid, R. A. Fischer, M. Hirscher, *Angew. Chem. Int. Ed.* **2013**, *52*, 13219–13222; c) S. Wan, J. Guo, J. Kim, H. Ihee, D. Jiang, *Angew. Chem. Int. Ed.* **2009**, *48*, 5439–5442; d) A. M. Evans, I. Castano, A. Brumberg, L. R. Parent, A. R. Corcos, R. L. Li, N. C. Flanders, D. J. Gosztola, N. C. Gianneschi, R. D. Schaller, W. R. Dichtel, *J. Am. Chem. Soc.* **2019**, *141*, 19728–19735; e) E. Hamzehpoor, C. Ruchlin, Y. Tao, C. H. Liu, H. M. Titi, D. F. Perepichka, *Nat. Chem.* **2023**, *15*, 83–90.

[5] C. Jia, R.-R. Liang, S.-X. Gan, S.-Y. Jiang, Q.-Y. Qi, X. Zhao, *Chem. Eur. J.* **2023**, *29*, e202300186.

[6] Y. Li, J. Ding, M. Day, Y. Tao, J. Lu, M. D′Iorio, *Chem. Mater.* **2003**, *15*, 4936–4943.

[7] G. H. Bertrand, V. K. Michaelis, T. C. Ong, R. G. Griffin, M. Dinca, *Proc. Natl. Acad. Sci. USA* **2013**, *110*, 4923–4928.

[8] S.-T. Yang, J. Kim, H.-Y. Cho, S. Kim, W.-S. Ahn, *RSC Adv.* **2012**, *2*, 10179–10181.

[9] S. B. Kalidindi, C. Wiktor, A. Ramakrishnan, J. Weßing, A. Schneemann, G. van Tendeloo, R. A. Fischer, *Chem. Commun.* **2013**, *49*, 463–465.

[10] E. Hamzehpoor, A. Jonderian, E. McCalla, D. F. Perepichka, *J. Am. Chem. Soc.* **2021**, *143*, 13274–13280.

[11] a) S. L. James, C. J. Adams, C. Bolm, D. Braga, P. Collier, T. Friščić, F. Grepioni, K. D. Harris, G. Hyett, W. Jones, A. Krebs, J. Mack, L. Maini, A. G. Orpen, I. P. Parkin, W. C. Shearouse, J. W. Steed, D. C. Waddell, *Chem. Soc. Rev.* **2012**, *41*, 413–447; b) A. Krusenbaum, S. Grätz, G. T. Tigineh, L. Borchardt, J. G. Kim, *Chem. Soc. Rev.* **2022**, *51*, 2873–2905.

[12] D. E. Crawford, *Beilstein J. Org. Chem.* **2017**, *13*, 65–75.

[13] T. Friščić, C. Mottillo, H. M. Titi, *Angew. Chem. Int. Ed.* **2020**, *59*, 1018–1029.

[14] a) M. Leonardi, M. Villacampa, J. C. Menéndez, *Chem. Sci.* **2018**, *9*, 2042–2064; b) A. C. Jones, J. A. Leitch, S. E. Raby-Buck, D. L. Browne, *Nat. Synth.* **2022**, *1*, 763–775; c) S. Grätz, D. Beyer, V. Tkachova, S. Hellmann, R. Berger, X. Feng, L. Borchardt, *Chem. Commun.* **2018**, *54*, 5307–5310; d) S. Grätz, B. Wolfrum, L. Borchardt, *Green Chem.* **2017**, *19*, 2973–2979; e) F. Effaty, X. Ottenwaelder, T. Friščić, *Curr. Opin. Green Sustain. Chem.* **2021**, *32*, 100524; f) K. J. Ardila-Fierro, J. G. Hernández, *Angew. Chem. Int. Ed.* **2024**, e202317638.

[15] a) C. Johnston, C. Hardacre, M. Migaud, *R. Soc. Open Sci.* **2021**, *8*, 201703; b) C. Bolm, J. G. Hernández, *ChemSusChem* **2018**, *11*, 1410–1420.

[16] a) T. Stolar, K. Užarević, *CrystEngComm* **2020**, *22*, 4511–4525; b) P. A. Julien, C. Mottillo, T. Friščić, *Green Chem.* **2017**, *19*, 2729–2747; c) P. Baláž, M. Achimovičová, M. Baláž, P. Billik, Z. Cherkezova-Zheleva, J. M. Criado, F. Delogu, E. Dutková, E. Gaffet, F. J. Gotor, R. Kumar, I. Mitov, T. Rojac, M. Senna, A. Streletskii, K. Wieczorek-Ciurowa, *Chem. Soc. Rev.* **2013**, *42*, 7571–7637; d) M. J. Rak, N. K. Saadé, T. Friščić, A. Moores, *Green Chem.* **2014**, *16*, 86–89; e) D. Tan, F. García, *Chem. Soc. Rev.* **2019**, *48*, 2274–2292; f) N. R. Rightmire, T. P. Hanusa, *Dalton Trans.* **2016**, *45*, 2352–2362; g) E. Boldyreva, *Chem. Soc. Rev.* **2013**, *42*, 7719–7738; h) V. Šepelák, A. Düvel, M. Wilkening, K.-D. Becker, P. Heitjans, *Chem. Soc. Rev.* **2013**, *42*, 7507–7520.

[17] C. Jimenez-Gonzalez, C. S. Ponder, Q. B. Broxterman, J. B. Manley, *Org. Process Res. Dev.* **2011**, *15*, 912–917.

[18] a) D. J. Am Ende, S. R. Anderson, J. S. Salan, *Org. Process Res. Dev.* **2014**, *18*, 331–341; b) A. A. L. Michalchuk, K. S. Hope, S. R. Kennedy, M. V. Blanco, E. V. Boldyreva, C. R. Pulham, *Chem. Commun.* **2018**, *54*, 4033–4036; c) H. M. Titi, J.-L. Do, A. J. Howarth, K. Nagapudi, T. Friščić, *Chem. Sci.* **2020**, *11*, 7578–7584; d) F. Effaty, L. Gonnet, S. G. Koenig, K. Nagapudi, X. Ottenwaelder, T. Friščić, *Chem. Commun.* **2023**, *59*, 1010–1013.

[19] a) A. Pichon, A. Lazuen-Garay, S. L. James, *CrystEngComm* **2006**, *8*, 211–214; b) T. Friščić, D. G. Reid, I. Halasz, R. S. Stein, R. E. Dinnebier, M. J. Duer, *Angew. Chem. Int. Ed.* **2010**, *49*, 712–715; c) Y.-H. Huang, W.-S. Lo, Y.-W. Kuo, W.-J. Chen, C.-H. Lin, F.-K. Shieh, *Chem. Commun.* **2017**, *53*, 5818–5821; d) M. Klimakow, P. Klobes, A. F. Thunemann, K. Rademann, F. Emmerling, *Chem. Mater.* **2010**, *22*, 5216–5221.

[20] B. P. Biswal, S. Chandra, S. Kandambeth, B. Lukose, T. Heine, R. Banerjee, *J. Am. Chem. Soc.* **2013**, *135*, 5328–5331.

[21] a) G. Das, D. B. Shinde, S. Kandambeth, B. P. Biswal, R. Banerjee, *Chem. Commun.* **2014**, *50*, 12615–12618; b) N. Brown, Z. Alsudairy, R. Behera, F. Akram, K. Chen, K. Smith-Petty, B. Motley, S. Williams, W. Huang, C. Ingram, X. Li, *Green Chem.* **2023**, *25*, 6287–6296.

[22] a) S. Hutsch, A. Leonard, S. Graetz, M. V. Hoefler, T. Gutmann, L. Borchardt, *Angew. Chem. Int. Ed.* **2024**, e202403649; b) S. T. Emmerling, L. S. Germann, P. A. Julien, I. Moudrakovski, M. Etter, T. Friščić, R. E. Dinnebier, B. V. Lotsch, *Chem* **2021**, *7*, 1639–1652; c) Y. Peng, G. Xu, Z. Hu, Y. Cheng, C. Chi, D. Yuan, H. Cheng, D. Zhao, *ACS Appl. Mater. Interfaces* **2016**, *8*, 18505–18512; d) D. B. Shinde, H. B. Aiyappa, M. Bhadra, B. P. Biswal, P. Wadge, S. Kandambeth, B. Garai, T. Kundu, S. Kurungot, R. Banerjee, *J. Mater. Chem. A* **2016**, *4*, 2682–2690; e) C. Zou, Q. Li, Y. Hua, B. Zhou, J. Duan, W. Jin, *ACS Appl. Mater. Interfaces* **2017**, *9*, 29093–29100; f) X. Wang, R. Ma, L. Hao, Q. Wu, C. Wang, Z. Wang, *J. Chromatogr. A* **2018**, *1551*, 1–9; g) G. Liu, H. Chen, W. Zhang, Q. Ding, J. Wang, L. Zhang, *Anal. Chim. Acta* **2021**, *1166*, 338539; h) Y. Yang, W. Zhao, H. Niu, Y. Cai, *ACS Appl. Mater. Interfaces* **2021**, *13*, 42035–42043; i) L. Gao, X. Zhao, S. Qin, Q. Dong, X. Hu, H. Chu, *Chirality* **2022**, *34*, 537–549; j) Y. Jiao, Y. Nan, Z. Wu, X. Wang, J. Zhang, B. Zhang, S. Huang, J. Shi, *Appl. Mater. Today* **2022**, *26*, 101381; k) N. Brown, Z. Alsudairy, R. Behera, F. Akram, K. Chen, K. Smith-Petty, B. Motley, S. Williams, W. Huang, C. Ingram, X. Li, *Green Chem.* **2023**, *25*, 6287–6296.

[23] Y. Tokunaga, H. Ueno, Y. Shimomura, *Heterocycles* **2002**, *57*, 787–790.

[24] T. Friščić, S. L. Childs, S. A. Rizvi, W. Jones, *CrystEngComm* **2009**, *11*, 418–426.

[25] In this work, COF_{BM} refers to any COF made via ball-milling, and COF_{RAM} refers to any COF made via Resonant Acoustic Mixing, unless noted otherwise.

[26] T. Ma, E. A. Kapustin, S. X. Yin, L. Liang, Z. Zhou, J. Niu, L.-H. Li, Y. Wang, J. Su, J. Li, X. Wang, W. D. Wang, W. Wang, J. Sun, O. M. Yaghi, *Science* **2018**, *361*, 48–52.

[27] N. R. Rightmire, T. P. Hanusa, *Dalton Trans.* **2016**, *45*, 2352–2362.

[28] Even though all mechanochemical techniques tested resulted in COF-1 formation (evidenced from its (110) reflection), only ball milling and RAM resulted in quantitative yields, as other techniques were challenged by insufficient mixing and fast evaporation of TMB.

[29] J. Gao, D. Jiang, *Chem. Commun.* **2016**, *52*, 1498–1500.

[30] a) S. D. Brucks, D. N. Bunck, W. R. Dichtel, *Polymer* **2014**, *55*, 330–334; b) D. N. Bunck, W. R. Dichtel, *Angew. Chem. Int. Ed.* **2012**, *51*, 1885–1889.

[31] a) I. Castano, A. M. Evans, H. Li, E. Vitaku, M. J. Strauss, J. L. Bredas, N. C. Gianneschi, W. R. Dichtel, *ACS Cent. Sci.* **2019**, *5*, 1892–1899; b) H. Li, A. M. Evans, W. R. Dichtel, J.-L. Bredas, *ACS Materials Lett.* **2021**, *3*, 398–405; c) R. L. Li, N. C. Flanders, A. M. Evans, W. Ji, I. Castano, L. X. Chen, N. C. Gianneschi, W. R. Dichtel, *Chem. Sci.* **2019**, *10*, 3796–3801;

d) H. Li, A. D. Chavez, H. Li, H. Li, W. R. Dichtel, J. L. Bredas, *J. Am. Chem. Soc.* **2017**, *139*, 16310–16318; e) B. Koo, R. Heden, P. Clancy, *Phys. Chem. Chem. Phys.* **2017**, *19*, 9745–9754; f) B. J. Smith, N. Hwang, A. D. Chavez, J. L. Novotney, W. R. Dichtel, *Chem. Commun.* **2015**, *51*, 7532–7535.

[32] a) T. Friščić, I. Halasz, P. J. Beldon, A. M. Belenguer, F. Adams, S. A. J. Kimber, V. Honkimäki, R. E. Dinnebier, *Nat. Chem.* **2012**, *5*, 66–73; b) C. B. Lennox, T. H. Borchers, L. Gonnet, C. J. Barrett, S. G. Koenig, K. Nagapudi, T. Friščić, *Chem. Sci.* **2023**, *14*, 7475–7481; c) A. A. L. Michalchuk, F. Emmerling, *Angew. Chem. Int. Ed.* **2022**, *61*, e202117270; d) G. M. Kuz'micheva, I. A. Kaurova, S. Brutti, C. Weidenthaler, *Crystals* **2022**, *12*, 345.

[33] X. Ma, T. F. Scott, *Commun. Chem.* **2018**, *1*, 98.

Manuscript received: March 5, 2024
Accepted manuscript online: July 5, 2024
Version of record online: September 20, 2024